

Trapping of Low-Level Internal Gravity Waves

N. ANDREW CROOK

Geophysical Fluid Dynamics Program, Princeton University, Princeton, New Jersey

(Manuscript received 22 June 1987, in final form 9 October 1987)

ABSTRACT

The characteristics of internal gravity waves propagating on a layer of high stratification near the ground with a deeper, weakly stratified layer above are examined with the aid of a nonhydrostatic numerical model. Simulations are performed of a density current propagating into an environment with a typically observed thermodynamic structure and with no shear. These simulations indicate that the amplitude of the disturbance that forms ahead of the density current is limited considerably by the upward propagation of energy in the upper layer.

To explain the large amplitude of observed gravity waves there must exist some additional mechanism, besides the weak stratification in the upper layer, to trap energy at low levels. A thorough examination of several observed gravity wave events suggested three commonly occurring mechanisms. The first mechanism, explored in a previous paper, occurs when winds in the upper layer oppose the wave motion. This reduces the Scorer parameter $l^2 = N^2/(U - c)^2 - U''/(U - c)$ in the upper layer and causes waves to evanesce in that region. The second mechanism, which also depends on a reduction in the Scorer parameter, occurs when a jet exists in the lower layer that opposes the wave motion. It is shown that the curvature in the velocity profile above this jet can produce a layer of negative Scorer parameter. Numerical simulations indicate that a considerable amount of energy can be trapped below this region of curvature.

The third mechanism involves an inversion at a certain height above the lower stable layer. In this system the Scorer parameter is actually increased, however for certain inversion heights energy can be reflected off the inversion and lead to an enhancement of the wave amplitude at the ground.

Observations of low-level internal gravity waves are then examined in an attempt to determine the relative importance of the three trapping mechanisms in the real atmosphere. This examination suggests that the low-level opposing flow is the most prevalent mechanism for trapping energy at low levels.

1. Introduction

The meteorological literature contains numerous reports of short-scale ($\lambda \sim 10$ km) gravity wave disturbances in which there is an initial pressure rise of the order of 1 ~ 2 mb followed by smaller amplitude waves. In these disturbances the surface pressure is generally greater after the passage of the waves than before; consequently the disturbances have been called atmospheric undular bores. Particularly well documented examples of the phenomena that will be discussed are the Morning Glory of northeastern Australia (see Clarke et al. 1981) and those reported by Potheary (1954), Schreffler and Binkowski (1981), Doviak and Ge (1984) and Haase and Smith (1984).

In the classical model of an undular bore propagating on, for example, the surface of a tidal river, the leading jump in surface height is followed by a train of surface waves that keep apace with the initial jump. For a given change in surface height the speed of the leading jump can be calculated from the conservation of mass and momentum (see Turner 1983, p. 67). The wavelength

of the following undulations can then be calculated by equating the bore speed with the speed of small amplitude surface gravity waves propagating on the deeper layer downstream (Benjamin and Lighthill 1954).

In a continuously stratified fluid like the atmosphere an undular bore is possible if strong stratification exists near the ground. However, any stratification above the lowest layers will allow energy to radiate in the vertical and limit the amplitude of the disturbance.

Although the process of upward energy radiation has been widely discussed in the literature we briefly review the subject here in order to gain an estimate of the decay rate of waves in a two-layer, continuously stratified fluid. The two-layer system is shown in Fig. 1 in a frame of reference in which the gravity waves are at rest.

The waves in this stratified system satisfy the Taylor-Goldstein equation

$$d^2w/dz^2 + m^2w = 0 \quad (1)$$

where

$$m^2 = N^2/(U - c)^2 - U''/(U - c) - k^2$$

or $m^2 = l^2 - k^2$; l^2 is often called the Scorer parameter ($U'' \equiv 0$ and $c \equiv 0$ for the simplified system in Fig. 1). In the upper layer the wave solution is of the form

Corresponding author address: Dr. N. Andrew Crook, Mesoscale and Microscale Meteorology Division, NCAR, P.O. Box 3000, Boulder, CO 80307.

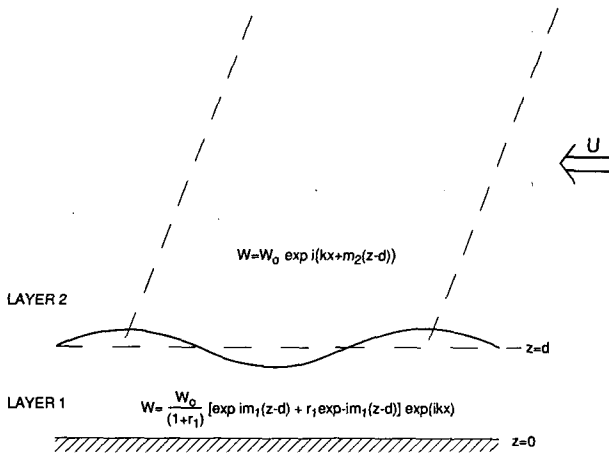


FIG. 1. Internal gravity wave propagating on a layer of high stability near the ground. A flow of speed U from the right has been imposed to bring the wave to rest. In the stable layer there is both an upward propagating mode and a downward mode; above the stable layer there is only the upward propagating mode (which has phase lines that tilt upstream with height).

$w = w_0 \exp i[kx + m_2(z - d)]$ where $m_2^2 = (N_2/U)^2 - k^2$. The wave solution in the lower layer is shown in Fig. 1. It is straightforward to show that the reflection coefficient r_1 must satisfy the conditions $r_1 = (m_1 - m_2)/(m_1 + m_2)$, (continuity of pressure), and $r_1 = -\exp(-2im_1d)$, (zero vertical velocity at the ground).

For upward energy propagation the lines of constant phase must slope upstream with height, hence we require that $m_2 < 0$. The upward flux of energy $F_z = \overline{p'w}$ (where the overbar represents an average over one wavelength) above the interface is given by (see, for example, Gill 1982, section 6.7)

$$F_z = \rho_0 U m_2 w_0^2 / 2k. \tag{2}$$

As energy is not being supplied to the system at the lower boundary the energy in the lower layer will be depleted at the rate given in Eq. (2). We can thus estimate a decay rate by dividing the total amount of wave energy in the lower layer by the upward flux of energy in the upper layer.

The total (kinetic and potential) wave energy E_t integrated over the depth d of the lower layer is

$$\overline{E}_t \approx 0.5 \left[0.5 \rho_0 \left(\frac{w_0}{\cos \phi} \right)^2 d \right] \tag{3}$$

where $\cos \phi = k/(k^2 + m_1^2)^{0.5} = (Uk)/N_1$ and we have made the approximation $m_2/m_1 \ll 1$ (which implies $r_1 \approx 1$ and $m_1 d \approx \pi/2$) since we are interested in the case of a weakly stratified layer (low m_2) above a strongly stratified layer (large m_1). In obtaining Eq. (3) we have made the long-wave approximation in the lower layer, i.e., $k^2 \ll m_1^2$ which is reasonable since the stratification is high in that layer. The overbar indicates integration over the depth of the lower layer and ϕ is the angle that the phase lines make with the vertical.

The reason that the integrated energy in the lower layer is approximately half that of a plane wave (see Gill 1982, section 6.7) is due to the interference of the upward propagating and downward propagating modes.

A decay rate can thus be estimated by dividing the integrated wave energy in the lower layer by the upward flux of energy F_z . Thus,

$$T_d \equiv \overline{E}_t / F_z \approx \frac{T_w}{8} \frac{N_1}{Um_2}. \tag{4}$$

We can simplify this further if we make the long-wave assumption in layer 2 also, i.e., $k^2 \ll m_2^2$. Then,

$$T_d \approx \frac{T_w}{8} \frac{N_1}{N_2}. \tag{5}$$

From the observations of the Morning Glory reported in Clarke et al. (1981), the ratio N_1/N_2 is typically around about 3 ~ 4. Thus $T_d < T_w$, i.e., the time scale for the decay of energy in the lower layer is less than the period of the wave. In other words, after one wave period (or, in this example, by the time air has traveled from one crest to the next) most of the energy has radiated away from the stable layer.

Thus, the basic question that we will attempt to answer in this paper is the following: Given that low-level gravity waves are often observed to propagate for several periods, what mechanisms exist that inhibit the radiation of energy away from the low levels?

The question of upward energy propagation has been examined in some detail in the context of gravity waves forced by the flow over mountains. Scorer (1949) showed that to obtain significant energy at the ground the term l^2 in Eq. (1) must decrease with height. In any layer where $l^2 < k^2$ (or equivalently $m^2 < 0$) the waves change from propagating in the vertical to decaying and hence energy in these wavelengths will be trapped below. Scorer (1949) solved analytically a two-layer system in which $(U - c)^2$ increased with height, and hence l^2 decreased, and suggested this as an explanation of the large amplitude gravity waves often observed in the lee of mountains.

In the context of undular bores a similar system has been examined by Crook (1986). Numerical simulations were performed of a density current propagating into a low-level stable layer and it was found that for environments in which the upper level winds oppose the wave motion [and hence where $(U - c)^2$ increases with height] considerable energy can be trapped in the stable layer. Evidence was presented to suggest that for Morning Glory's that propagate from the northeast $(U - c)^2$ does indeed increase with height since the upper level winds are usually westerly.

Many of the other reported instances of low-level gravity waves however do not occur in environments in which the upper level winds oppose the wave motion. An extensive examination of many of these gravity wave events suggested two further mechanisms that

can trap energy at low levels. The first involves the presence of a low level jet that opposes the wave motion. As will be shown the curvature in the wind profile above the jet can produce a layer in which the Scorer parameter changes sign.

The second mechanism which is particularly relevant for the Morning Glory is the presence of an inversion at around 3–4 km. This mechanism which has previously been examined in the context of mountain waves (Klemp and Lilly 1975) does not involve a reduction in the Scorer parameter but depends on wave reflection off the inversion.

In the present paper we present numerical simulations of density currents propagating into environments that include low level jets (section 3b) and inversions (section 3c) in order to examine their effectiveness in trapping wave energy. We then examine a number of observed gravity wave events in an attempt to classify the relative importance of these mechanisms in the real atmosphere.

2. The numerical model

The numerical model used is a two-dimensional, dry, anelastic, nonhydrostatic model derived from the three-dimensional cloud model described in Lipps and Hemler (1982). The subgrid scale mixing terms have been modified from Lipps and Hemler (1982) to allow for the effects of reduced mixing in regions of higher stability and for any anisotropy in the grid spacing.

The horizontal gridlength Δx is 600 m, the vertical gridlength $\Delta z = 120$ m. There are 80 points in the vertical and 170 in the horizontal. A damping function similar to that used in Crook (1986) is specified in the upper 30 levels. Several test simulations were performed to determine the optimum strength of the damping function. It was found that a damping time of 4 min at the midlevel of the damping layer gave the most efficient damping of waves in the upper levels of the model.

In Crook and Miller (1985) and Crook (1986) a density current was formed in the domain by specifying an inflow of cold air at the left hand boundary. Once the density current had moved a sufficient distance into the domain the air at low levels ahead of the current was cooled to form a stable layer. An undular bore disturbance was then generated as the current collided with this layer of increased stability. This interaction process was viewed as a model of the generation of the Morning Glory, which forms when a strong sea breeze from the northeast coast of Australia collides with a layer of high stability in the region of the Gulf of Carpentaria. (This layer of high stability may itself be part of a sea breeze, or "gulf" breeze, circulation from the Gulf of Carpentaria.)

In the present work bore disturbances are generated in a somewhat different manner. The model is initialized with a stable layer that extends the width of the

domain. A density current is then formed by specifying a heat sink near the ground which cools air continuously for the duration of the simulation. The density current then intrudes into the stable layer and if the conditions are correct, a bore disturbance will propagate ahead of the current. To a certain extent this models the system that occurs when a thunderstorm forms above a low-level stable layer. When the evaporatively cooled air in the thunderstorm reaches the ground, it spreads out into the layer of high stability and for certain conditions can push a bore disturbance ahead.

The simulations to be examined are summarized in Table 1.

3. Results

a. High stability at low levels, weaker above (un-sheared)

The stable layer used in all of the simulations is 780 m deep and has a potential temperature difference of 10°C across it, giving a gradient of 13°C km^{-1} . The heat sink is 1 km deep and 12 km wide. The analytical form used for the heat sink is a step function in both vertical and horizontal directions and takes a value for all simulations (except run 6) of $0.5^\circ\text{C min}^{-1}$. In Fig. 2 the potential temperature field at $t = 90$ min is shown for two simulations. In simulation 1 there is no stratification above the lower layer. In simulation 2 the upper layer is stratified with a lapse rate of $1.7^\circ\text{C km}^{-1}$ (which gives a Brunt-Väisälä period of 14 min). This is a fairly typical value from the observations of the Morning Glory and similar undular bore disturbances.

The effect of vertical energy propagation is clearly visible. In the simulation without upper level stratification two large amplitude waves have propagated ahead of the density current and a third is beginning to form above the head of the current. The maximum vertical velocity in the leading wave has reached a value of 2.4 m s^{-1} after 90 min. In the simulation with stratification in the upper level, two waves have also moved ahead of the current and a third is forming at the density current's head. However, the amplitude of these waves is very small, the maximum vertical velocity being 0.2 m s^{-1} after 90 min.

TABLE 1. Simulation parameters.

Run 1:	Stable layer 780 m deep, 10° potential temperature difference, unstratified above. Unsheared. Heat sink $0.5^\circ\text{C min}^{-1}$.
Run 2:	As in Run 1 except stratification above stable layer = $1.7^\circ\text{C km}^{-1}$.
Run 3:	As in Run 2 except with the low level wind shown in Fig. 3a by the solid line.
Run 4:	As in Run 2 except with the low level wind shown in Fig. 3a by the dashed line.
Run 5:	As in Run 2 except with a constant wind of -5 m s^{-1} specified throughout domain.
Run 6:	As in Run 3 except with 1°C min^{-1} cooling in heat sink.
Run 7:	As in Run 2 except with inversion of 8° centered at 3.7 km.

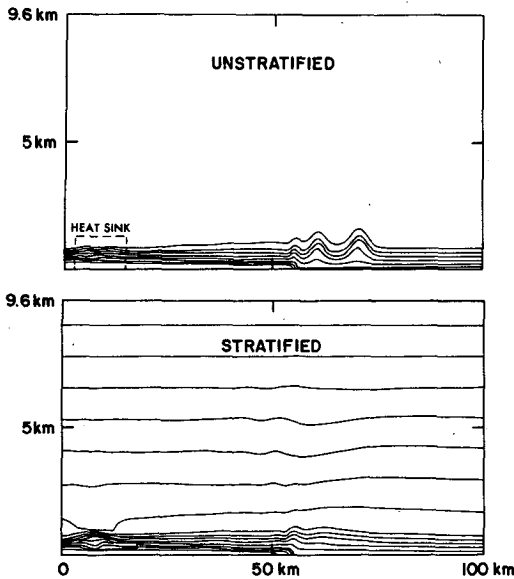


FIG. 2. (a) The potential temperature field for run 1 after 90 min (contour interval 2°C). The position of the heat sink is shown by the dashed lines. (b) The potential temperature field for run 2 (at $t = 90$ min). The lapse rate in the upper layer is $1.7^\circ\text{C km}^{-1}$.

In the unstratified case the wavespeed is 11.3 m s^{-1} , the wavelength (defined as the distance between the first two crests) is 9.7 km, and hence the period of the dominant wave is 14.3 min. In the case with upper level stratification the small amplitude oscillation at low levels has a wavespeed of 9.9 m s^{-1} and wavelength of 7.9 km. Hence for these waves $m_2^2 = N_2^2/U^2 - k^2 = -6.5 \times 10^{-8} \text{ (m}^{-2}\text{)} < 0$ which means that the disturbance at this wavelength of 7.9 km is trapped in the vertical. This leads to an important question concerning the present work, viz, why it is difficult to obtain significant energy in a disturbance which has a dominant wavelength with $m^2 < 0$. To answer this we first note that for the disturbance in simulation 1 there is not only energy in the dominant wavelength (i.e., given by the distance between the first and second crests) but a substantial amount of energy at longer wavelengths. This is both because the wave disturbance is limited in the horizontal direction and also because the downstream depth of the stable layer is greater than the upstream depth. For these longer wavelengths $m_2^2 > 0$ so that energy is able to propagate into the upper layer. The results of simulations 1 and 2 show that the upward energy propagation in these longer wavelengths is enough to limit substantially the growth of any bore disturbance. These longer wavelengths that have propagated into the upper layer are clearly evident in the potential temperature field in Fig. 2b and also in the vertical velocity field for an equivalent experiment shown in Fig. 2a of Crook (1986).

To obtain a significant amount of energy at low levels it is necessary to include additional complexity in the idealized two-layer environment of simulation 2. We

now examine one commonly occurring mechanism that traps energy at low levels—that of an opposing low level jet.

b. Opposing low level jet

In a large number of the reported instances of short-scale internal gravity waves the flow at low levels (below $\sim 1 \text{ km}$) is in the opposite direction to the wave motion. A particularly well documented example is that reported by Doviak and Ge (1984). The wind field (observed by both tall tower and Doppler radar) parallel to the wave motion is shown in Fig. 5c of their study and is reproduced in Table 2 of the present work. The wind below 700 m opposes the wave motion with a maximum velocity of approximately 7 m s^{-1} at 500 m. Above 700 m, the ambient flow is in the same direction as the wave motion with a local maximum of 5 m s^{-1} existing at around 1 km.

The reason that a wind profile of the form of that reported by Doviak and Ge can trap energy at low levels is shown in Fig. 3. The term m^2 , or equivalently the Scorer parameter [Eq. (1)], not only depends on the stratification but also on the curvature of the wind profile. For the profiles shown in Fig. 3a the wind curvature below the zero wind level increases the Scorer parameter and thus assists in wave propagation. Above the zero wind level the curvature is of the opposite

TABLE 2. Observations of low-level internal gravity waves.

DISTURBANCE	HIGH STRATIFICATION AT GROUND LOW ABOVE N_2	OPPOSING UPPER LEVEL FLOW	OPPOSING LOW LEVEL FLOW	INVERSION
NORTHEASTERLY MORNING GLORY 10 October 1981	Yes $N_2/N_1=0.27$	Yes	Yes 	Yes 7°/100m at 4km
SOUTHERLY MORNING GLORY	Yes $N_2/N_1=0.3$	No	No	Yes
MISSOURI DISTURBANCE Shreffler and Binkowski (1981)	Yes $N_2/N_1=0.38$	No	Yes 	No
OKLAHOMA Haase and Smith (1984)	Yes $N_2/N_1=0.45$	No	Yes 	No
OKLAHOMA Doviak and Ge (1984)	Yes $N_2/N_1=0.34$	No	Yes 	Slight 2°/100m at 2.5km
ENGLAND Potchary (1954)	Yes $N_2/N_1=0.3$	No	Yes 	Yes 5°/400m at 1.5km

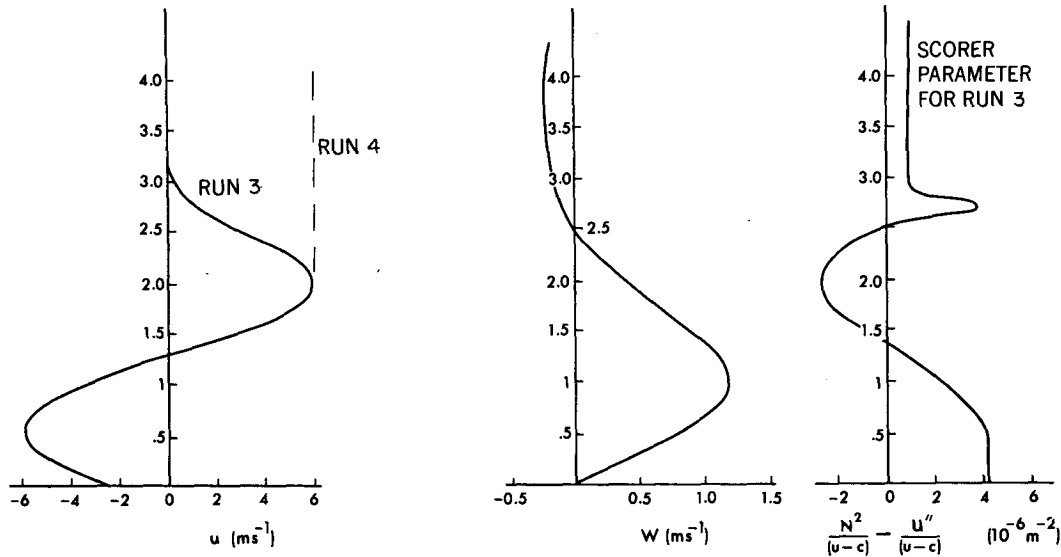


FIG. 3. (a) Ambient wind profile for run 3 and run 4. In run 3 the curvature in the wind profile goes to zero above 3.2 km. In run 4 the wind curvature vanishes above 2 km. (b) The vertical velocity in the leading wave for run 3. (c) The Scorer parameter upstream of the disturbance in run 3. Note the layer of negative values between 1.4 and 2.5 km.

sense, hence, the Scorer parameter is reduced. As is shown in Fig. 3c, the Scorer parameter can change sign in this region and thus can provide a substantial amount of energy trapping.

To examine this effect further we integrate the numerical model with the same potential temperature profile as in experiment 2 but specify a low-level flow below 3 km. To explore the sensitivity to the exact nature of the wind profile two experiments are performed with wind profiles that differ in the region above the zero wind level. For the first profile (run 3) the wind velocity returns to zero above 3.2 km, for the second profile (run 4) the wind velocity remains at a constant positive value above 2 km (see Fig. 3a).

The combination of stable layer and the wind profile shown in Fig. 3a may at first appear rather specific. However, in most density driven flows (for instance katabatic wind, sea breeze, thunderstorm outflow) there exists a low level jet with return flow above. In other words, flow profiles of the form shown in Fig. 3a are not uncommon when a layer of cold air exists at low levels.

The potential temperature and vertical wind fields for experiment 3 are shown in Fig. 4. A disturbance with a maximum vertical velocity of 1.3 m s^{-1} can be seen propagating ahead of the density current. The bore speed (8.4 m s^{-1}) and the distance between the first and second crests (7.4 km) are reduced somewhat compared to simulations 1 and 2.

The results of experiment 4 (in which the wind curvature is zero above 2 km) are very similar to those of experiment 3. The bore speed is the same (8.4 m s^{-1}) whereas the wavelength is slightly increased to 7.9 km. As the curvature of the wind profile vanishes above 2

km the degree of trapping is slightly less in experiment 4 than in experiment 3. For this reason the maximum vertical velocity at $t = 90 \text{ min}$ in experiment 4 is reduced by approximately 30% (to 0.95 m s^{-1}) compared to experiment 3.

The vertical velocity in the leading wave in experiment 3 is plotted in Fig. 3b alongside the vertical profile of the Scorer parameter, Fig. 3c. The vertical velocity

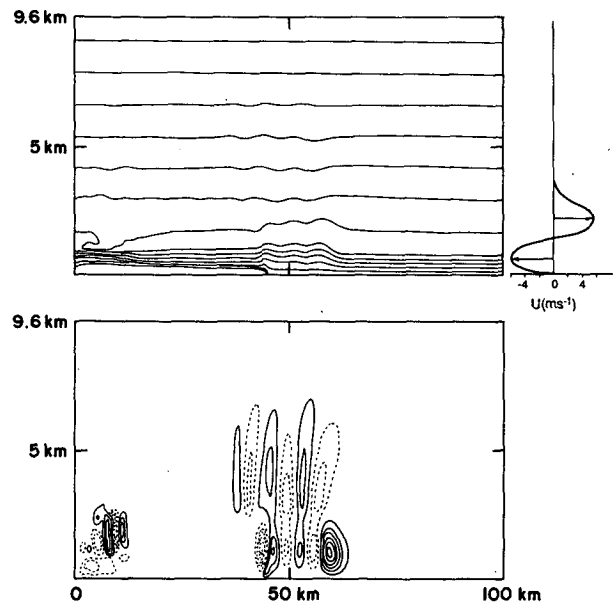


FIG. 4. (a) The potential temperature field at $t = 90 \text{ min}$ for run 3 (contour interval 2°C). (b) The vertical velocity field at the same time for run 3 (contour interval 0.2 m s^{-1}).

goes rapidly to zero in the region where the Scorer parameter is negative indicating that the region of reverse curvature above the low level jet is important for trapping energy below. Further downstream the mean potential temperature and mean horizontal wind profiles are altered by the action of the bore. To conserve mass, the velocity at low levels in the bore is increased (becomes less negative) whereas above the bore the velocity is decreased. The trapping characteristics of the flow downstream of the leading jump are hence altered and as can be seen from the vertical velocity field in Fig. 4b this allows more energy to propagate upwards.

It could be argued that the large response in experiment 3 is simply a reflection of the increased convergence that has been produced by specifying winds that oppose the motion of the density current. Laboratory experiments, numerical results and the analytical model described in Crook (1984) show that a larger density current (with a consequent large horizontal convergence at the nose) generates a stronger bore moving ahead of it. We can show, however, that the large amplitude of the disturbance in experiment 3 is a result of the curvature above the low level flow and not simply a result of the increase in horizontal convergence by running an experiment with an opposing flow which has no curvature.

In Fig. 5 the potential temperature field at $t = 120$ min is shown for an experiment which uses the same cooling rate as before but with an opposing flow of 5 m s^{-1} specified throughout the depth of the domain (run 5). The density current in this experiment moves at approximately the same speed as in experiment 3 (4.2 m s^{-1}), hence, the horizontal convergence between density current and upstream flow is approximately the same. A "wedge" of cold air is pushed ahead of the density current; however, very little energy is trapped at low levels, the maximum vertical velocity in the disturbance ahead of the current being less than 0.2 m s^{-1} .

The author's attention has recently been drawn to a study by Rotunno et al. (1988) that bears some relation to the present work. Following the previous study by Thorpe et al. (1982) they examine the importance of a low level jet in the maintenance of long-lived squall lines. Rotunno et al. find a similar result to that previously found by Thorpe et al., viz., that a squall line persists for considerably longer in an environment that includes a low level jet. Rotunno et al. argue that the increase in lifetime is due to the fact that the *shear* in the low level jet results in an *increase* in the *vertical velocity* at the nose of the density current and demonstrate this by performing several density current simulations in various shear strengths.

In the present study, in which the low level flow is highly stratified, we have found a similar result in that before the first gravity wave leaves the density current the vertical velocity at the nose of the current is greatly increased in the presence of the low level flow. In this

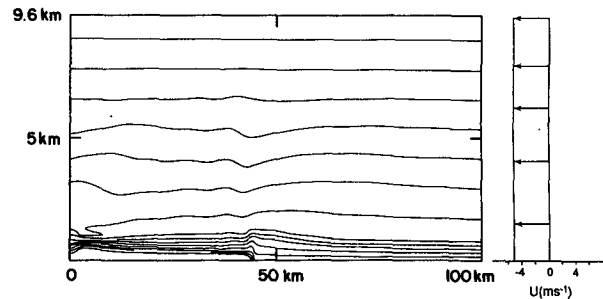


FIG. 5. The potential temperature field at $t = 120$ min for run 5 (constant velocity field of -5.0 m s^{-1}) (contour interval 2°C).

section we have invoked the variation of the Scorer parameter to interpret this result and argued that it is the region of reverse curvature that necessarily must exist above a low level shear flow that traps energy below it.

However the present study differs from that of Rotunno et al. in that we have included stratification in the low level flow and this allows the region of large vertical velocity to move ahead of the density current in the form of gravity waves. Intriguingly however, the two studies may be related by the observation that the large amplitude gravity waves observed by Doviak and Ge (1984) and others usually propagate from a region where severe *long-lived* convection existed some hours earlier.

We conclude this section by demonstrating the efficiency of low level wind curvature in trapping energy by running an experiment with a stronger density current. An experiment was run with the same potential temperature and wind profile as in experiment 3 but with the cooling rate in the heat sink doubled to 1°C min^{-1} (see Fig. 6). A very large disturbance can be seen ahead of the density current with the maximum vertical velocity in the initial wave reaching 5.0 m s^{-1} after 120 min.

c. The effect of an inversion

A further mechanism for trapping energy is suggested by the numerical results of Clarke (1984). With a hydrostatic model Clarke examined the behavior of colliding sea breeze fronts and used an observed thermodynamic profile which contained a strong inversion at around 3 km. These strong inversions which are frequently observed in the region that the Morning Glory occurs (the observations of Smith and Morton 1984 show an 8°C temperature difference in 100 m) are most likely a result of strong subsidence in the descending branch of the Hadley circulation.

To examine the effect that an inversion of this strength can have on low-level gravity waves we integrate the numerical model with an inversion specified above the low-level stable layer. In Fig. 7 the potential

temperature field (at $t = 66$ and 90 min) is shown for an experiment with the same initial profile as simulation 2 except with a highly stratified layer centered about 3.7 km. This layer is 360 m deep with a potential temperature difference of 8°C across the layer.

As can be seen after 90 min two waves have moved ahead of the density current and a third is beginning to form above the head of the current. The maximum vertical velocity in the leading wave is 1.1 m s^{-1} (which is about one-half that in simulation 1 but an order of magnitude greater than in experiment 2). The propagation speed of the bore is 10.5 m s^{-1} , dominant wavelength 9.6 km and hence the period of the dominant wave is 15.3 min.

Gravity waves of significant amplitude are also evident propagating on the inversion. The waves on the inversion can be separated into two modes: those propagating above the undular bore at low levels (and at the same speed as the bore) and those propagating above (and at the same speed as) the density current. The fact that the bore moves ahead of the density current is nicely illustrated by the fact that the waves above the bore have a greater horizontal wavelength than the waves above the density current (recalling that for nonhydrostatic internal gravity waves the wave speed increases with increasing horizontal wavelength).

The increase in amplitude of the disturbance in the stable layer when an inversion is included can be explained in the following manner (for a more quantitative explanation, see Gill 1982, section 6.9.1). Due to reflection off the lower interface of the inversion there is not only an upward propagating mode in the weakly stratified region between the stable layer and the inversion but also a downward mode. If this weakly stratified region is one quarter of a vertical wavelength deep then the upward propagating and downward mode will interfere *destructively* at the base of the inversion to give a minimum in wave amplitude there. Thus the response forced in the inversion and, consequently, the upward propagation of energy will be reduced to a minimum. Furthermore if the *inversion* depth is one quarter of a wavelength, then the upward

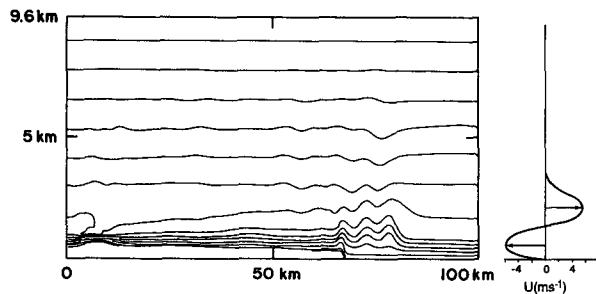


FIG. 6. The potential temperature field at $t = 120$ min for run 6 (wind field the same as run 3, cooling in heat sink = $1^\circ/\text{min}$) (contour interval 2°C).

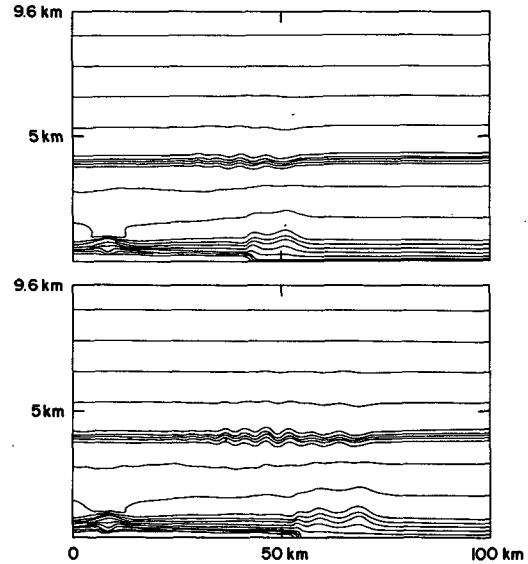


FIG. 7. The potential temperature field for run 7 at (a) $t = 66$ min and (b) $t = 90$ min (contour interval 2°C).

and downward modes *in the inversion* will interfere destructively at the *upper* interface of the inversion to give a minimum in wave amplitude there. Hence the response in the region above the inversion will be reduced to a minimum.

To summarize, the upward propagation of energy is minimized if the weakly stratified region below the inversion is one quarter of a vertical wavelength deep. The upward propagation will be further reduced if the inversion depth is also one quarter of a vertical wavelength. Unfortunately this condition is complicated by the fact that the vertical wavelength $2\pi/m$ depends on the horizontal wavelength [see Eq. (1)]. Thus, the optimal height for the inversion varies with horizontal wavelength and as already discussed the bore consists of a spectrum of these wavelengths.

However we can estimate the optimal height of the inversion for the dominant wave in Fig. 7. As already noted this wave has $\lambda = 9.6$ km and $U - c = 10.5 \text{ m s}^{-1}$. In the weakly stratified region $N^2 = 5.5 \times 10^{-5} \text{ (s}^{-2}\text{)}$ hence $m = [N^2/(U - c)^2 - k^2]^{0.5} = 0.27 \times 10^{-3} \text{ (m}^{-1}\text{)}$. This gives a quarter vertical wavelength of $\lambda/4 = \pi/(2m) = 5.7$ km. The depth of the weakly stratified region is 3 km, hence a deeper layer would give more reflection of the dominant wave. However the longer wavelengths (smaller k) that are also present in the bore disturbance have shorter vertical wavelengths and hence will be closer to the optimal value for reflection.

A similar calculation can be carried out for the inversion layer. As the stratification is large in this layer, we can make the long wave assumption, hence $m = N/U = 2.7 \times 10^{-2}/10.5 = 2.6 \times 10^{-3} \text{ (m}^{-1}\text{)}$. This gives a quarter vertical wavelength of $\lambda/4 = \pi/(2m) = 610$ m. As the inversion in simulation 7 is 360 m deep, it is

clear that a stronger or deeper inversion would give more reflection, and this holds for all horizontal wavelengths. However the occurrence in nature of stronger inversions than that used in simulation 7 (8°C in 360 m) is presumably quite rare.

4. Observations of long-lived gravity waves

We conclude this study by examining a number of observations of long-lived gravity waves (with periods of ~ 10 min) to determine the relative importance of the trapping mechanisms discussed above and in Crook (1986). The disturbances to be examined are the northeasterly Morning Glory, the southerly Morning Glory, and those reported in other parts of the world by Doviak and Ge (1984), Shreffler and Binkowski (1981), Haase and Smith (1984), and Potheary (1951).

Numerous observations of northeasterly Morning Glories have been reported in the literature. These observations could be ensemble averaged to obtain a mean condition under which northeasterly Morning Glories are observed. However, averaging in this way tends to "smear" out the intense vertical gradients of potential temperature and wind which are important in trapping energy at low levels. For this reason we shall examine just one Morning Glory from the northeast for which the predisturbance conditions were fairly typical, (the well documented example of 11 October 1981, Smith and Morton 1984).

Observations of southerly Morning Glories are more scarce than those from the northeast. As these disturbances usually occur in the same season (spring) as their northeasterly counterpart it is reasonable to assume that the environment in the middle to upper troposphere will be similar to that on days on which northeasterly disturbances occur. As far as the lower level conditions are concerned a study by Smith et al. (1986) of four southerly disturbances showed that there was no pronounced low level flow towards these disturbances (see their Fig. 7).

The observations are summarized in Table 2. As shown in the second column all of the disturbances propagate on a layer of high stability near the ground with a weakly stratified, almost neutral, layer above. The ratio, N_2/N_1 is approximately 0.3 for all of the disturbances giving a ratio of lapse rates in the two layers, (N_2^2/N_1^2) , of approximately 1 to 10.

In the next three columns the trapping mechanisms discussed above are listed, i.e., opposing upper level flow, opposing low level flow and inversion. Against each observed disturbance the existence (or nonexistence) of the three trapping mechanisms is listed. In the second last column (opposing low level flow) the velocity profile in the direction of wave motion up to about 2 km is shown for each disturbance. (A negative value indicates a velocity opposing the wave motion.) Unfortunately, only a few wind measurements are available for the disturbance reported by Potheary (1954).

As can be seen all three mechanisms exist for the northeasterly Morning Glory which undoubtedly is part of the reason why gravity wave disturbances are so commonly observed in northern Queensland moving from this direction. For southerly Morning Glories the only trapping mechanism present is the upper level inversion.

Also as can be seen, for the disturbances examined, the first mechanism of opposing upper level flow is only important for the northeasterly Morning Glory.

The final point to note about Table 2 is that the second mechanism (opposing low level flow) exists for all disturbances, except the southerly Morning Glory. Furthermore, for four of the disturbances, the two described in Shreffler and Binkowski (1981) and the two in Oklahoma, the *only* trapping mechanism is the opposing low level flow which demonstrates the importance of that mechanism for the maintenance of short scale gravity waves.

5. Conclusions

In this paper we have examined the propagation characteristics of short period (~ 10 min) gravity waves on a layer of high stability near the ground. It has been shown for a case in which the Brunt-Väisälä period is 5 min in the stable layer and 14 min above (and with no shear in the environment) that the upward flux of energy in the upper layer severely limits the amplitude of disturbances that can form at low levels.

To explain the amplitude and lifetime of observed gravity wave disturbances it is necessary to include additional complexity in the idealized environment described above. The first method of increasing the amplitude and lifetime of low level gravity waves is to specify opposing winds above approximately 4 km, (discussed in Crook 1986).

The second method of trapping energy is to specify a jet in the stable layer opposing the wave motion. The important feature of this mechanism is the region of reverse curvature that must exist above the low level flow. This produces a negative Scorer parameter which can trap energy below.

The third method of trapping energy at low levels is to specify an inversion at approximately 4 km. A numerical simulation showed that the amplitude of the disturbance at low levels can be increased by an order of magnitude by including a strong inversion. The increase in amplitude is due to wave reflection off the lower and upper interfaces of the inversion. Maximum reflection occurs when both the layer below the inversion and the inversion itself are one quarter of a vertical wavelength deep.

Several observed gravity wave disturbances have been examined to explore the existence of these trapping mechanisms. For Morning Glories that propagate from the northeast all three mechanisms are present. In several of the other observations examined the only

trapping mechanism present was the low level opposing flow.

Acknowledgments. The author would like to thank the following for helpful discussions: I. Orlanski, F. Lipps, R. Pierrehumbert and R. Rotunno. The figures were drafted by P. G. Tunison and staff. The financial support given by the Geophysical Fluid Dynamics Program at Princeton University under NOAA Grant NA84-EAD00057 is gratefully acknowledged.

REFERENCES

- Benjamin, T. B., and M. J. Lighthill, 1954: On cnoidal waves and bores. *Proc. Roy. Soc. London*, **A224**, 448–460.
- Clarke, R. H., 1984: Colliding sea breezes and the creation of internal atmospheric bore waves: Two-dimensional numerical studies. *Aust. Meteor. Mag.*, 207–226.
- , R. K. Smith and D. Reid, 1981: The Morning Glory of the Gulf of Carpentaria. At atmospheric undular bore. *Mon. Wea. Rev.*, **109**, 1733–1757.
- Crook, N. A., 1984: The formation of the Morning Glory. *Mesoscale Meteorology—Theories, Observations and Models*. D. K. Lilly, and T. Gal-Chen, Eds., 349–353.
- , 1986: The effect of ambient stratification and moisture on the motion of atmospheric undular bores. *J. Atmos. Sci.*, **43**, 171–181.
- , and M. J. Miller, 1985: A numerical and analytical study of atmospheric undular bores. *Quart. J. Roy. Meteor. Soc.*, **111**, 225–242.
- Doviak, R., and R. Ge, 1984: An atmospheric solitary gust observed with a Doppler radar, a tall tower and a surface network. *J. Atmos. Sci.*, **41**, 2559–2573.
- Gill, A., 1982: *Atmosphere-Ocean Dynamics*. Int. Geophys. Ser. Vol. 30, Academic Press.
- Haase, S., and R. K. Smith, 1984: Morning Glory wave clouds in Oklahoma: A case study. *Mon. Wea. Rev.*, **112**, 2078–2089.
- Klemp, J. B., and D. K. Lilly, 1975: The dynamics of wave-induced downslope winds. **32**, 320–339.
- Lipps, F. B., and R. S. Hemler, 1982: A scale of deep moist convection and some related numerical calculations. *J. Atmos. Sci.*, **39**, 2192–2210.
- Pothecary, I. J. W., 1954: Short period variations in surface pressure and wind. *Quart. J. Roy. Meteor. Soc.*, **104**, 543–567.
- Rotunno, R., J. B. Klemp and M. L. Weisman, 1988: A theory for severe long lived squall lines. *J. Atmos. Sci.*, in press.
- Scorerer, R. S., 1949: Theory of waves in the lee of mountains. *Quart. J. Roy. Meteor. Soc.*, **75**, 41–56.
- Shreffler, J. H., and F. S. Binkowski, 1981: Observations of pressure jump lines in the Midwest. *Mon. Wea. Rev.*, **109**, 1713–1725.
- Smith, R. K., and B. R. Morton, 1984: An observational study of northeasterly “morning glory” wind surges. *Aust. Meteor. Mag.*, 155–175.
- , M. J. Coughlan and J. L. Lopez, 1986: Southerly nocturnal wind surges and bores in northeastern Australia. *Mon. Wea. Rev.*, **114**, 1501–1518.
- Thorpe, A. J., M. J. Miller and M. W. Moncrieff, 1982: Two-dimensional convection in nonconstant shear: A model of mid-latitude squall lines. *Quart. J. Roy. Meteor. Soc.*, **108**, 739–762.
- Turner, J. S., 1983: *Buoyancy Effects in Fluids*. Cambridge University Press.